J.Mycopathol.Res. 63(4) : 753-762, 2025, ISSN : 0971-3719 (Print), 2583-6315 (Online)

10.57023/JMycR.63.4.2025.753

Bacterial Hsp90 proteins: a potential drug target against plant pathogenic bacteria

ANINDYA BISWAS*, ALOKE MANDAL AND ANKITA CHOWDHURY
[1]Plant-microbe Interaction Laboratory, Department of Botany, Siksha Bhavana (Institute of Science), Visva-Bharati, Santiniketan-731235, West Bengal

Received : 11.08.2025 Accepted : 25.10.2025 Published : 29.12.2025

Heat shock protein 90 (Hsp90) is a ubiquitous and essential protein among prokaryotes and eukaryotes. It plays a critical role as a molecular chaperone under optimal and stress-induced cellular conditions by promoting folding, remodeling, and stabilization of cellular proteins,facilitating optimal maintenance of cellular events. Plant pathogenic bacteria cause various plant diseases in economically important crops, resulting in severe global agro-economic losses. Our study includes *in silico* characterization of bacterial Hsp90 proteins encoded by bacterial phytopathogens that indicates Hsp90 encoded by alpha, beta, and gamma proteobacteria differ in sequence similarity and are distantly placed from Hsp90 encoded by fungi, plants, and humans in the phylogenetic tree. Further studies demonstrated that Hsp90 encoded by different plant pathogenic bacteria have more or less similar physicochemical properties, secondary structural elements, domain organization, and tertiary conformation as monomer and dimer. Predicted 3D structures and molecular docking studies identified the conserved amino acid residues involved in ADP binding and dimerization. Our study suggests that phytopathogenic bacteria encode for Hsp90 proteins that can be a suitable target for any naturally derived small druggable molecules, and it can be an effective measure for controlling plant pathogenic bacteria,avoiding the usage of antibiotics in agriculture in the future.

Keywords : Heat shock protein 90, plant pathogenic bacteria, protein folding, Drug target

INTRODUCTION

Heat shock protein 90 (Hsp90) has been considered a highly conserved and abundant protein (0.5-2% of total cellular protein) in bacteria and eukaryotes under normal cellular conditions. However, the expression of Hsp90 is upregulated under different environmental stress conditions,including elevated temperature, non-physiological pH, availability of oxygen, etc. to mitigate cell damage (Harris *et al.* 2004; Wickner*et al.* 2021). It acts as an ATP-dependent molecular chaperon that functions in proteostasis by facilitating folding, remodeling, and often activation of other unfolded or misfolded cellular proteins,leading to protein stabilization and the fundamental events of cell survival in bacterial and eukaryotic cells (Shiau *et al.* 2006; Wickner*et al.* 2021). Additionally, Hsp90 often protects cellular proteins from aggregation and degradation to maintain their cellular function and the optimal functioning of the cell. However, bacterial Hsp90 interacts with DnaK, the bacterial homolog of Hsp70, which collaborates with a J-domain protein (JDP) and a nucleotide exchange factor (NEF) for optimal functioning. However, Bacterial Hsp90 plays a critical role in cellular, metabolic, and physiological function, which differs in the structural organization and sequence homology from eukaryotic Hsp90 (Wickner*et al*. 2021). Different plant pathogenic bacteria also express Hsp90 proteins that act as an essential regulator for governing virulence-associated function and stress responses (Figaj, 2025).

Microbial phytopathogens cause significant agro-economic losses around the world. A large number of bacterial species represent a significant contributor as potential phytopathogens. Approximately 200 different species belonging to the Kingdom Monera have been reported to cause major plant diseases in economically important crops (Buttimer *et al*. 2017).Bacterial diseases in major crops cause considerable losses in crop yield, quality, and

*Correspondence : anindya.biswas@visva-bharati.ac.in

related economy (Mulungu, 2024). For example, the yield of round potato, an important crop round the world, encounters significant loss only in India, China, East and Central Africa, ranging from 10-100% due to *Ralstonia solanacearum* infection (Jiang *et al*. 2017; Munyaneza and Bizimungu, 2022; Tessema and Seid, 2023). Likewise, *R. solanacearum* infection global economic loss of about 848 million USD (Wang *et al*. 2023).The usage of antibiotics in agriculture against plant pathogenic bacteria has been limited due to concern about the emergence of antimicrobial resistance (Islam *et al*. 2024). Exploration of novel antibacterial strategies is needed to control plant diseases caused by bacterial phytopathogens effectively. Introduction of small druggable molecules against specific, conserved, and essential cellular components of bacterial phytopathogens can be effective and has fewer chances to develop antimicrobial resistance.

Our present study, on the basis of *in silico* exploration, has made structural and functional characterization of Hsp90 proteins encoded by different plant pathogenic bacteria. Hsp90 proteins are highly conserved among the bacterial phytopathogens, but structurally distinct from those of the eukaryotic Hsp90, including plants. Our study suggeststhat Hsp90 encoded by potential plant pathogenic bacteria can be a potential drug target useful in agriculture without hampering ecological balance and chances of antimicrobial resistance.

MATERIALS AND METHODS

Retrieval of protein sequences of Hsp90 proteins

A total of 10 different Hsp90 (gene product of *htpG*) sequences of different plant pathogenic bacteria were retrieved from UniProt database (https://www.uniprot.org/) listed in Table 1. Respective gene sequences and genetic organization were retrieved and demonstrated according to IMG database(https://img.jgi.doe.gov/)and BV-BRC 3.53.3 database (https://www.bv-brc.org/).

Physiochemical properties and subcellular localization of Hsp90

Different physicochemical properties, including molecular weight (M.W.), extinction coefficient (EC), isoelectric point (pI), aliphatic index (Ai), instability index (Ii), grand average of hydrophobicity (GRAVY) of Hsp90s were analyzed using ExPasy Prot Protein Param tool (https://web.expasy.org/protparam/)(Gasteiger *et al*. 2005; Haan *et al*. 2021).All this computed information has been listed in Table1.

Secondary structure analysis

Secondary structural elements of retrieved Hsp90 proteins were analyzed by the secondary structure prediction server Jpred 4(https://www.compbio.dundee.ac.uk/jpred/). It was further studied by PDBsum (https://www.ebi.ac.uk/thornton-srv/databases/pdbsum/).Additionally, secondary structural analysis, including the possible amount of α-helices, extended strand, β-turns, coils were done by SOPMA from the Network Protein Sequence Analysis server https://npsa-prabi.ibcp.fr/cgi-bin/npsa_automat.pl?page=/NPSA/npsa_sopma_f.html) (Gasteiger *et al*. 2005; Haan *et al*. 2021).

Tertiary structure analysis

The three-dimensional(3D) monomeric and dimeric model structures of Hsp90 proteins of different plant pathogenic bacteria along with bound Mg^{2+} and adenosine diphosphate (ADP) were builtwith AlphaFold 3.0 (https://alphafoldserver.com/) and best energy-minimized structures were selected for further study (Abramson*et al*. 2024).PyMol was used for visualization, analysis, and publishable image creation of the built structures (PDB files). Predicted 3D models of both monomeric and dimeric proteins were evaluated using the SAVES server 6.1 (https://saves.mbi.ucla.edu/). Respective Ramachandran Plots were generated using RAMPLOT server (https://www.ramplot.in/). Domain organization of the respective 3D models was predicted by aligning them with *E. coli* Hsp90 ADP-bound PDB structure (PDB ID: 2IOP). The results were further confirmed with CDD-NCBI and UniProt databases.

Protein interaction network analysis

Protein-protein interaction network of retrieved Hsp90 proteins (Hsp90-AT, Hsp90-RS, and Hsp90-XO) and exploration of cellular protein-

protein interaction network were analyzed using STRING 12.0 (https://string-db.org/). Graphical representation of the Confidence score (C score) generated by STRING was made using GraphPad Prism software v8.

Multiple sequence alignment

Clustal Omega algorithm (https://www.ebi.ac.uk/jdispatcher/msa/clustalo)was used for the alignment of retrieved Hsp90 sequences and respective amino acid sequences of their putative N-terminal domains (NTD) through multiple sequence alignment.

Phylogenetic analysis

Phylogenetic tree was constructed from retrieved amino acid sequences of bacterial Hsp90 encoded by different plant pathogenic bacteria following the Maximum Likelihood method with 1000 bootstrap value using MEGA-X software to decipher the evolutionary relationship of the taxa. Another phylogenetic tree was made comparing the evolutionary relatedness of bacterial Hsp90 with different eukaryotic Hsp90 proteins following the Maximum Likelihood method with 1000 bootstrap values using MEGA-X software. It was further computed and represented as a circular phylogenetic tree using iTol v7 (https://itol.embl.de/).

Molecular docking study

The 3D structure of Hsp90 Proteins (Hsp90-AT, Hsp90-RS, Hsp90-XO) were used for molecular docking with the 3D model of ADP (downloaded from the PubChem database (http://pubchem.ncbi.nlm.nih.gov/) using AutodockVina programv1.1.2 in Linux platform (Ubuntu v24.04.1 LTS), following a standard protocol (Mahato *et al*. 2025). Prior to docking, the protein molecule was prepared using UCSF Chimerav1.19. There were no water molecules,co-crystallizing ligand in the protein molecule. Therefore,hydrogen atoms were added,Gasteiger charges were assigned,and ensured that there were no unbound atoms in the protein. The ADP was also prepared in UCSF chimera, where hydrogen atom was added and charges were assigned similarly. The docking was executed by specifying the Hsp90 as the receptor and the ADP as aligand. The best binding pose was selected bythe UCSF Chimera based on the higher binding affinity (in kcal/mol) and lower RMSD value,which determines the best orientation within the active site. The Receptor Ligand complex was further analyzed and validated by Biovia Discovery Studio,where the 2D figures were also generated.

RESULTS AND DISCUSSION

Most bacterial phytopathogens possess single copy of Hsp90-encoding gene

Heat shock protein (Hsp90) is a highly conserved ATP-dependent molecular chaperone protein. It is usually comprised of three domains, the N-terminal domain (NTD), the middle domain (MD), and the C-terminal domain (CTD) (Fig. 1a).It usually exists as a homodimer. It bears an ATP/ADP-independent form (*apo*) that can undergo conformational changes by ATP hydrolysis, and interaction with cochaperons, and substrate proteins to achieve its active *holo* conformation reversibly (Fig.1a).In the present study, the amino acid sequences of Hsp90 proteins encoded by different plant pathogenic bacteria were retrieved from Unit Prot database. Plant pathogenic bacteria are represented by a limited number of bacterial generalike *Agrobacterium, Burkholderia, Dickeya, Erwinia, Pantoea, Pectobacterium, Pseudomonas, Ralstonia, Xanthomonas,* and *Xylella,* which are well-studied as bacterial plant pathogens.Among these genera,certainpotent plant pathogenic species capable of causing devastating diseases in economically important crops worldwide have been selected as the experimental model *in silico* in this study. A group of plant pathogenic bacteria restrict their host to a specific plant,where as a certain other group of bacteria can cause disease in a wide range of plants. *Burkholderia glumae* causes bacterial panicle blight in rice crop, a seed-borne bacterial major disease, in different countries of Asia, Africa, North and South America (Zhou-qi *et al*. 2016). Likewise, *Xanthomonas oryzae* causes bacterial leaf blight disease, a major devastating disease for agro-economic loss in rice worldwide (Verma *et al*. 2020). Both of these rice pathogenic bacteria are included in this study as representative of their respective genus. Similarly, *Erwinia amylovora* is one of the well-studied

bacterial phytopathogens that causes the fire blight disease in apple were considered to represent its genus (Kharadi*et al*. 2021). However, *Xylella fastidiosa* has been initially found to be associated only with the Pierce's Disease in grapes; later, it has been reported to be involved in numerous symptomatic as well as asymptomatic diseases in a wide range of plants in Europe and America are also included as a representative of its genus (Sicard *et al*.2018).In contrast, *Agrobacterium tumefaciens* and *Pantoeaananatis,* and *Ralstonia solanac-earum,* which cause diseases in a wide range of host plants, causing crown gall disease and bacterial wilt disease, respectively, were also included (Coutinho and Venter, 2009; Genin and Denny, 2012; Gohlke and Deeken, 2014). The study also includes a number of soft-rot causing bacterial species like *Dickeya dadantii* and *Pectobacterium carotovorum,* which infect a wide range of economically important host plants,causing soft rot symptoms (Jiang *et al*. 2022; Maisuria and Nerurkar, 2013).

Our study revealed that most of the genera representing bacterial phytopathogens, other than *Xanthomonas,* possess a single copy of *htp G*gene (encodes for Hsp90) in their genome. Interestingly, different strains of *Xanthomonas* possess two *htp G*genes that encode for two distinct Hsp90s which differ from each other in their amino acid sequences. However, *X. oryzae* pv. *oryzae* strain KACC10331 possesses one *htpG* present solitarily in the genome, but its paralog is present in the genome within an operon along with two other genes (Fig.1b). Interestingly, the rest of the plant pathogenic bacteria belonging to other genera do not exhibit any *htpG* gene solitarily. However, the genetic organization of *htpG* and its neighbouring genes under the same operon can be distinct. *P. syringae* exhibits the occurrence of *htpG* along with a different gene(Fig.1b). However, the genetic organization of *htpG* in *D. dadantii, E. amylovora, P. ananatis,* and *P. carotovorum* is more or less similar, along with seven neighbouring genes under the same promoter (Fig.1b).Similarly, *B. glumae* and *R. solanacearum* exhibit similar genetic organization of *htpG* along with four other neighbouring genes under the same promoter, but those are distinct from that of the *X. oryzae* pv. *oryzae, P. syringae, D. dadantii, E. amylovora, P. ananatis,* and *P. carotovorum* (Fig.1b).

Hsp90 differ in their sequence phylogenetically

A horizontal phylogenetic tree was constructed through MEGA-X using the retrieved amino acid sequences of bacterial Hsp90 proteins encoded by plant pathogenic bacteria considered for this study. The phylogenetic tree [Figure 1c] exhibits the presence of two different clades representing the clustering of the members of beta proteobacteria (*B. glumae and R. solanaceraum*) and the members of gamma proteobacteria (*D. dadantii, E. amylovora, P. ananatis, P. carotovorum, P, syringae, X. oryzae,* and *X. fastidiosa*). The clades of beta and gamma proteobacteria are distantly placed from *A. tumefaciens,* a member of alpha proteobacteria (Fig.1c).The horizontal branches represented evolutionary lineages whereas the longer branches represent the elevated change among the organisms (Hasan *et al*. 2021). The result indicates that despite critical sequence homology, bacterial Hsp90 proteins differ according to their classes (alpha, beta, or gamma proteobacteria). However, further analysis in this study has exhibited a comparative representation of three Hsp90 proteins, Hsp90-AT, Hsp90-RS, and Hsp90-XO from *A. tumefaciens, R. solanacearum,* and *X. oryzae,*considering them as the representatives of alpha, beta, and gamma proteobacterial plant pathogenic bacteria, respectively.

The circular phylogenetic tree represents the evolutionary relationship between Hsp90 proteins encoded by Gram positive and Gram-negative bacteria including different plant and animal pathogenic bacteria, and different eukaryotic Hsp90 proteins including Hsc82 encoded by fungi (*Saccharomyces cerevisiae*), AtHsp90-1 encoded by plant (*Arabidopsis thaliana*), and mammalian Hsp90α and TRAP1 (mitochondrial Hsp90) encoded by human (Fig.1d).The result indicates all plant and animal pathogenic bacteria belonging to gamma proteobacteria are placed together but differ from alpha and beta proteobacteria members. However, eukaryotic Hsp90s are placed distantly compared to

bacterial Hsp90 proteins. Interestingly, Hsp90 encoded by *Mycobacterium tuberculosis* was in the same clade with the member of alpha proteobacteria (*A. tumefaciens*), whereas another Gram-positive bacterium,*Bacillus subtilis* is placed closely with TRAP1 found in human mitochondria. The phylogenetic analysis indicates that Hsp90 encoded by plant pathogenic bacteria is distantly related to eukaryotic Hsp90, including fungi, plants, and mammals.

Hsp90 encoded by bacterial phytopathogens possesses similar physicochemical properties and secondary structural organization

The retrieved amino acid sequences were analysed through ExPASy Prot Param tool, and the results have been listed in Table1. The analysis unveiled that most of the bacterial phytopathogens encode for Hsp90 proteins possessing 630-640 amino acid residues, and the molecular weight of the Hsp90 monomers ranges between 69-72 kDa. Most of the proteins are slightly acidic in nature (pI ranges between 4.86 to 5.31) (Table 1) and can be considered as stable according to their instability index (Table 1). Additionally, all of the Hsp90 proteins can be regarded as hydrophilic in nature based on their GRAVY index (Table 1). However, Hsp90 proteins encoded by different plant pathogenic bacteria from alpha, beta, and gamma proteobacteria are almost similar in their physicochemical properties.

The secondary structural analysis of the retrieved amino acid sequences of Hsp90 encoded by different plant pathogenic bacteria through Jpred 4 and PDBsum exhibited that the secondary structural organization of the Hsp90s is almost similar (data not shown). Further, SOPMA analysis using NPS@ server revealed that Hsp90s harbour predominantly alpha helical structures (about 49-53%), followed by about 13-14% beta strand, 6-8% beta turns, and 26-30% random coils (Table2). Fig.2a exhibits the distribution of the secondary structural elements in different domains in the Hsp90-AT, Hsp90-RS, and Hsp90-XO. This analysis also showed that different plant pathogenic bacteria belonging to alpha, beta, and gamma proteobacteria harbour almost similar domain-wise distribution of secondary structural elements.However, eukaryotic Hsp90 proteins comprise a charged linker between NTD and MD, and often the CTD contains a highly conserved MEEVD motif at the termini, which are lacking in the bacterial Hsp90 (Li *et al*. 2024).

Hsp90 interacts with different other cellular proteins

A protein-protein interaction network analysis was performed using STRING database, and the interaction networks corresponding to Hsp90-AT, Hsp90-RS, and Hsp90-XO are represented in Fig.2b and summarized in Fig.2c. Interacting proteins bearing a higher confidence score (C score), with values ranging from 0 to 1 and increasing with a greater correlation, are considered highly interactive (Mahato *et al*. 2025). The protein-protein interaction network of studied plant pathogenic bacterial Hsp90 proteins indicates that all of them typically interact with their respective co-chaperons like DnaJ and DnaK [Fig2b &2c].Additionally, plant pathogenic Hsp90 is shown to interact with other chaperons like GroEL, HslU, HslV, along with other 16 organism-specific interacting partners essential for various cellular functions [Fig 2b &2c].

Hsp90 encoded by bacterial phytopathogens exists as a homodimer

Possible monomeric and dimeric 3D models of Hsp90-AT, Hsp90-RS, and Hsp90-XO were prepared through AlphaFold 3.0 (Abramson *et al*. 2024) and visualized through Pymol [Figure 3a].All the structures have been validated through the structure validation server SAVES 6.1 with ERRAT, Verify3D, and PROCHECK tools. These tools have been considered globally as essential for proper validation, accuracy, and quality check of the predicted 3D models of protein molecules (Yadav et al. 2013).3D models of other Hsp90s from other plant pathogenic bacteria were also prepared (data not shown) and analysed in similar way, summarized in the (Table3). The ERRAT score of Hsp90_AT, Hsp90-RS, and Hsp90-XO has been calculated as 97.5934, 96.1353 and 97.6518, respectively,which depicts the quality of the generated 3D models (Table3). The structure validation algorithm of ERRAT interprets the overall quality of the predicted 3D model (Hasan

et al. 2021). The Verify3D analysis exhibited all of the model structures have been passed as per the quality standard (Table3). Verify3D considers at least 80% of the amino acids to have scored e" 0.2 in the 3D/1D profile as acceptable. The predicted 3D models were finally validated through Ramachandran plot generated through PROCHECK and Ramplot, which depicts the model structures harbouring all amino acid residues are present within the favoured region and G-factor represents their overall quality assessment (Table3). It is evident that 90% of the amino acids in the Ramachandran plot's favored region are considered characteristics of a good quality model structure (Hasan *et al*. 2021). In monomeric structures of the Hsp90 proteins, the NTD, MD, and CTD domains have been shown as blue, orange, and red regions, respectively. In dimeric structures, it has been demonstrated as a homodimer where two chains (two monomers) interact, leading to a *holo* conformation of Hsp90. Domain organization in dimeric structures has been exhibited with different colour codes (Fig3). Mg^{2+} (shown as red) and ADP (shown as green) were incorporated as ligands (shown with red arrow) in both monomeric and dimeric structures of the respective Hsp90 proteins (Fig.3a-c).

Different domains of Hsp90 are involved in different functions

The 3D models deciphered that ADP is bound to the N-terminal domain (NTD) of the bacterial Hsp90 proteins. PDBsum analysis further revealed that the amino acid residues present in MD and CTD are responsible for dimerization of the monomeric subunits through specific hydrogen bonding, salt bridges, and non-bonded interactions (Table4).The interaction between the Hsp90 proteins and ADP was further analysed through molecular docking study that showed ADP binds to the N-terminal domain of the bacterial Hsp90 proteins and interacts with specific conserved amino acid residuesin bacterial Hsp90 proteins encoded by alpha, beta, and gamma proteobacterial plant pathogenic bacteria (Fig.4a&4b). It indicates helices H2,H5, and H7 present in the NTD are involved in ADP binding. Molecular docking study further unveiled the binding affinity of the ADP molecule (ligand) to bacterial Hsp90 proteins (Table 5).The result

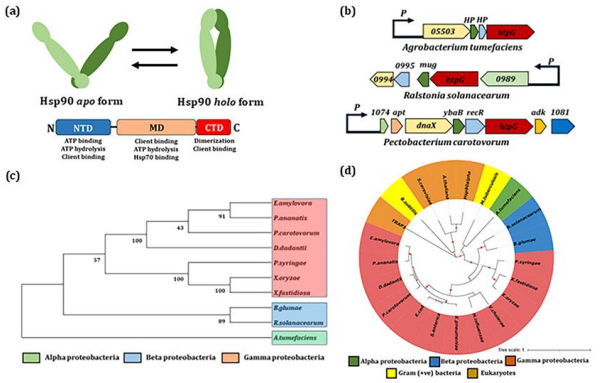

Fig. 1 : (a) Domain organization and reversible conformational changes of Hsp90 in *apo* and *holo* form. (b) Genetic organization of *htpG* gene (encodes for Hsp90) in *A. tumefaciens, R. solanacearum,* and *P. carotovorum,*representing alpha, beta, and gamma proteobacteria, respectively. (c) Phylogenetic tree showing the position and evolutionary relationship of plant pathogenic bacteria belonging to alpha, beta, and gamma proteobacteria, in terms of Hsp90. (d) Circular phylogenetic tree showing the position and evolutionary relationship of plant pathogenic bacteria with other eukaryotic Hsp90 proteins.

shows Hsp90-AT, Hsp90-RS, and Hsp90-XO exhibit the binding affinities towards ADP of about -8.4, -9.2, and -7.9 kcal/mole, respectively; which seems more or less similar.

Our present study demonstrated that most of the plant pathogenic bacteria, infecting a variety of economically important plants, encode for bacterial Hsp90 protein, which is placed in different clades according to their belonging to different classes, like alpha, beta, and gamma proteobacteria. The genetic organization of *htpG* gene along with its neighbouring genes and operons is also different among alpha, beta, and gamma proteobacteria members. It indicates the genetic regulation and expression of Hsp90 might be governed in a different way in alpha, beta, and gamma proteobacteria. Interestingly, most of them encode for a single copy of *htpG* gene, whereas only different strains of *Xanthomonas* encode for two copies of *htpG* gene,which differ in genetic organization and sequence homology. Hsp90 plays a significant role in regulating essential cellular, metabolic, and physiological functions and is one of the critical regulators of virulence and stress responses in plant pathogenic bacteria (Figaj, 2025).However, our study also showed that Hsp90 encoded by plant pathogenic bacteria differs significantly in sequence homology, domain organization, and phylogenetic position from that of the eukaryotic Hsp90 encoded by fungi, plants, and mammals.

Table 1: Physiochemical properties of Hsp90 proteins encoded by different plant pathogenic bacteria

Plant pathogenic bacteria	Name	UniProtKb	Amino acid residues	Molecular Weight	pI	Instability index	Aliphatic index	GRAVY
Agrobacterium tumefaciens	Hsp90-AT	A0AA44F4I3	630	69874.82	5.13	35.27	85.67	-0.344
Burkholderia glumae	Hsp90-BG	A0AAP9Y268	632	71344.29	5.17	35.44	85.55	-0.496
Dickeya dadantii	Hsp90-DD	E0SDX0	627	71407.95	4.92	38.36	82.63	-0.546
Erwinia amylovora	Hsp90-EA	D4HYJ4	624	71082.98	5.00	38.42	83.21	-0.514
Pantoea ananatis	Hsp90-PA	A0A0H3KXR0	624	71051.89	4.97	38.83	85.24	-0.496
Pectobacterium carotovorum	Hsp90-PC	A0A419AVL6	629	71468.11	4.86	39.09	83.15	-0.511
Pseudomonas syringae	Hsp90-PS	A0A1C7Z3K4	635	71316.71	5.18	39.02	88.33	-0.441
Ralstonia solanacearum	Hsp90-RS	A0AA92JT15	640	71410.55	5.18	32.42	89.39	-0.371
Xanthomonas oryzae	Hsp90-XO	A0AAP0ZH02	634	70783.86	5.17	36.53	88.49	-0.424
Xylella fastidiosa	Hsp90-XF	Q9PEQ0	635	71765.18	5.31	35.57	88.89	-0.444

Table 2 : Secondary structure analysis of Hsp90 proteins encoded by different plant pathogenic bacteria

Plant pathogenic bacteria	Name	Alpha Helix	Extended Strand	Beta turn	Random Coil
Agrobacterium tumefaciens	Hsp90-AT	49.12%	13.81%	6.98%	29.68%
Burkholderia glumae	Hsp90-BG	51.42%	13.45%	7.91%	27.22%
Dickeya dadantii	Hsp90-DD	52.15%	13.72%	7.34%	26.79%
Erwinia amylovora	Hsp90-EA	52.88%	13.46%	7.37%	26.28%
Pantoea ananatis	Hsp90-PA	52.77%	13.53%	7.54%	26.33%
Pectobacterium carotovorum	Hsp90-PC	52.31%	13.51%	7.63%	26.55%
Pseudomonas syringae	Hsp90-PS	51.50%	13.39%	7.4%	27.72%
Ralstonia solanacearum	Hsp90-RS	52.34%	13.44%	7.19%	27.03%
Xanthomonas oryzae	Hsp90-XO	51.89%	13.88%	7.73%	26.5%
Xylella fastidiosa	Hsp90-XF	52.12%	13.81%	7.54%	26.53%

Table 3 : Validation of predicted 3D structures of Hsp90 encoded by different plant pathogenic bacteria

Proteins	ERRAT	Verify3D	PROCHECK (through Ramachandran Plot)			G-Factor (Overall Average)
			Most favored region	Additional allowed region	Generously allowed region	Disallowed region	
Hsp90-AT	97.5934	Pass	93.6%	6.4%	0.0%	0.0%	0.14
Hsp90-BG	94.2904	Pass	94.9%	4.9%	0.2%	0.0%	0.18
Hsp90-DD	93.4534	Pass	95.0%	5.0%	0.0%	0.0%	0.19
Hsp90-EA	94.281	Pass	96.2%	3.8%	0.0%	0.0%	0.18
Hsp90-PA	94.6254	Pass	95.5%	4.5%	0.0%	0.0%	0.18
Hsp90-PC	94.599	Pass	94.7%	5.3%	0.0%	0.0%	0.18
Hsp90-PS	97.7273	Pass	95.8%	4.2%	0.0%	0.0%	0.17
Hsp90-RS	96.1353	Pass	95.0%	5.0%	0.0%	0.0%	0.18
Hsp90-XO	97.6518	Pass	95.2%	4.7%	0.1%	0.0%	0.16
Hsp90-XF	97.3422	Pass	92.9%	6.7%	0.3%	0.0%	0.14

Table 4 : Details of interaction between two monomers in different Hsp90 homodimers

Proteins	Chain A		Chain B		Type of Interactions		
	Number of residues	Interface Area	Number of residues	Interface Area	Hydrogen bonds	Non-bonded contacts	Salt bridges
Hsp90-AT	81	4295	81	4307	49	449	6
Hsp90-BG	75	3910	76	3906	34	395	10
Hsp90-DD	83	4061	84	4058	38	397	2
Hsp90-EA	45	2429	46	2438	24	215	1
Hsp90-PA	83	4235	84	4250	45	431	7
Hsp90-PC	81	3925	81	3932	42	438	2
Hsp90-PS	82	4357	83	4357	50	471	8
Hsp90-RS	64	3567	35	3549	30	408	8
Hsp90-XO	81	4295	81	4307	49	449	6
Hsp90-XF	78	4173	79	4162	44	408	5

Table 5: Details of protein-ligand interaction between ADP and different Hsp90

Proteins	Interacting domain	Ligand	Binding energy
Hsp90-AT	NTD	ADP	-8.4 kcal/mol
Hsp90-RS	NTD	ADP	-9.2 kcal/mol
Hsp90-XO	NTD	ADP	-7.9 kcal/mol

It suggests bacterial Hsp90 harbours certain unique structural features that distinguish it structurally from eukaryotic Hsp90, and this feature can be the most significant parameter to consider bacterial Hsp90 as a possible drug target that might not be able to interact with eukaryotic Hsp90.Moreover, our study unveiled that the Hsp90 comprises similar primary, secondary, and tertiary structural organization in the members of alpha, beta, and gamma proteobacteria. 3D structural analysis and molecular docking study also deciphered that the NTD is responsible for interaction with nucleotides (ADP/ATP), whereas the MD and CTD are involved in the oligomerization. So, it is evident that bacteria Hsp90 exhibits more or less conserved structural organization,though different plant pathogenic bacteria were placed distantly in their respective phylogenetic tree.In agriculture, prevention and control measures against plant pathogenic bacteria are still less effective, though these microbial pathogens cause huge agro-economic losses worldwide. Antibiotics are less recommended for agricultural applications due to concerns about the emergence of antimicrobial resistance. Under such circumstances, small molecules targeting different conserved but essential bacterial cellular components can be an alternative, safer, and effective strategy against plant pathogenic bacteria.On this account, various small molecules derived from natural resources, including bacterial, fungal, or plant resources, having Hsp90 inhibitory activity can be applied in optimal concentration. Several naturally derived Hsp90 inhibitors, which belong to quinones, terpenoid derivatives, resorcinol, pyrazoles, isoxazoles, triazoles, pyrimidine, benzamides, benzothiazoles,benzofurans, etc.,have already been characterized (Li *et al*. 2024). Among them, some molecules like some specific Novobiocin-derivatives are reported to bindto NTD of eukaryotic Hsp90 (Li *et al*. 2024). Some of the druggable small molecules disrupt client protein binding to the MD domain, like Deguelin derived from bark, roots, and leaves of certain leguminous plants like *Mundulea sericea*, *Derris montana*, and *Tephrosia vogelii* (Wang *et al*. 2013). Likewise, a number of naturally derived small molecules like Vibsane-type diterpenes isolated from *Viburnum* plantscan interact with the CTD of eukaryotic Hsp90 for its inhibition (Li *et al*. 2024).However, naturally derived Hsp90 inhibitors like Fusicoccin-A (derived from fungus, *Phomopsis amygdali*) should be avoided for agricultural applications as recent studies revealed it can hamper different physiological functions of plants (de Boer, 2024). Various naturally derived druggable molecules should be explored computationally and experimentally, targeting different conserved regions of bacterial

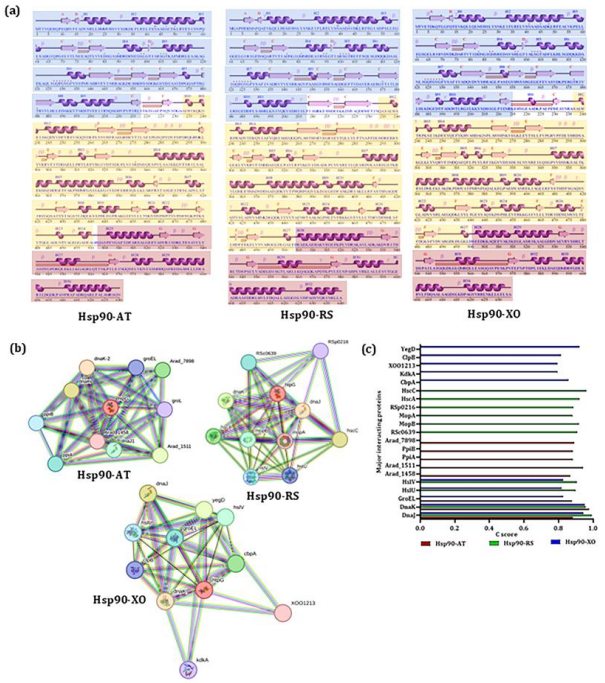

Fig. 2 : (a) Domain-wise distribution of secondary structural elements in Hsp90 encoded by *A. tumefaciens, R. solanacearum,* and *X. oryzae*. (b) Protein-protein network analysis generated by STRING. (c) Graph showing C value of protein-protein interaction generated by STRING.

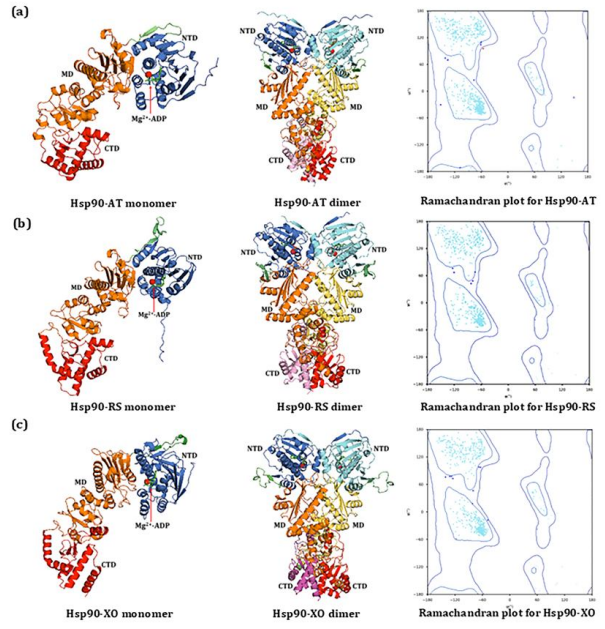

Fig. 3: (a-c) Monomeric and dimeric three-dimensional structures (predicted and generated by AlphaFold 3.0), along with respective Ramachandran plots of Hsp90-AT, Hsp90-RS, and Hsp90-XO.

Hsp90 to inhibit Hsp90 function that can lead us to develop effective strategy for successfully eliminating plant pathogenic bacteria.

ACKNOWLEDGEMENTS

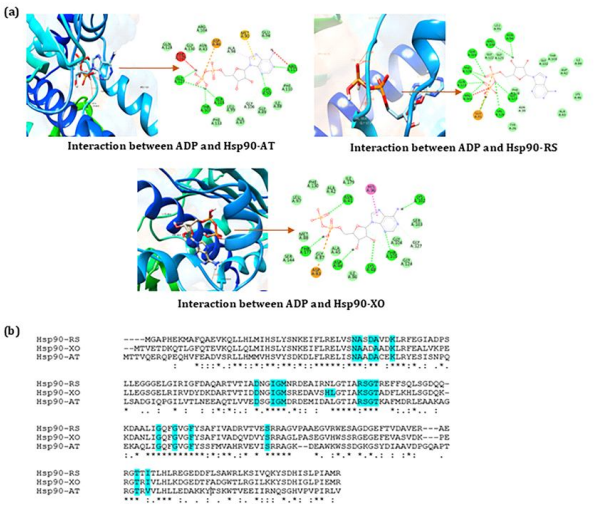

Fig 4 : (a) Molecular interaction between ADP and Hsp90 proteins (generated by molecular docking) showing interacting amino acid residues (Deep green denotes hydrogen bonding and light green denotes van der Waals interaction). (b) Multiple sequence alignment of Hsp90-AT, Hsp90-RS, and Hsp90-XO showing (blue) interacting amino acid residues responsible for ADP-binding.

AM and AC are the recipients of the non-NET fellowship provided by UGC. This study was supported by DST-INSPIRE Faculty Research Grant from DST, Govt. of India to AB

DECLARATION

Conflict of Interest. Authors declare no conflictof interest.

REFERENCES

Abramson, J., Adler, J., Dunger, J., Evans, R., Green, T., Pritzel, A., ... Jumper, J. M. 2024. Accurate structure prediction of biomolecular interactions with AlphaFold 3. *Nature***630**: 493-500.doi.org/10.1038/s41586-024-07487-w

Buttimer, C., McAuliffe, O., Ross, R. P., Hill, C., O'Mahony, J., Coffey, A. 2017. Bacteriophages and bacterial plant diseases. *Front.Microbiol*. **8**: 34.doi.org/10.3389/fmicb.2017.00034

Coutinho, T. A.,Venter, S. N. 2009. *Pantoeaananatis*: an unconventional plant pathogen. *Mol.Plant Pathol*. **10**: 325-335.doi.org/10.1111/j.1364-3703.2009.00542.x

de Boer, A. H. 2024. The fusicoccin story revisited. *J.Exper. Bot*. **75**: 5531-5546.doi.org/10.1093/jxb/erae300

Figaj, D. 2025. The role of heat shock protein (Hsp) chaperones in environmental stress adaptation and virulence of plant pathogenic bacteria. *Inter. J. Mol. Sci*. **26**: 528.doi: 10.3390/ijms26020528

Gasteiger, E., Hoogland, C., Gattiker, A., Duvaud, S. E., Wilkins, M. R., Appel, R. D.,Bairoch, A. 2005. Protein identification and analysis tools on the ExPASy server. In :*The proteomics protocols handbook* (N.J. Totowa)pp. 571-607. Humana press.doi.org/10.1385/1-59259-890-0:571

Genin, S., Denny, T. P. 2012. Pathogenomics of the *Ralstonia solanacearum* species complex. *Annu.Rev.*

Phytopathol. **50**: 67-89.doi.org/10.1146/annurev-phyto-081211-173000

Gohlke, J.,Deeken, R. 2014. Plant responses to Agrobacterium tumefaciens and crown gall development. *Front. Plant Sci*. **5**: 155.doi.org/10.3389/fpls.2014.00155

Harris, S. F., Shiau, A. K.,Agard, D. A. 2004. The crystal structure of the carboxy-terminal dimerization domain of htpG, the Escherichia coli Hsp90, reveals a potential substrate binding site. *Structure*, **12**: 1087-1097.DOI: 10.1016/j.str.2004.03.020

Hasan, R., Rony, M. N. H.,Ahmed, R. 2021. In silico characterization and structural modeling of bacterial metalloprotease of family M4. *J.Genet.Engineer. Biotechnol*. **19**: 25.doi.org/10.1186/s43141-020-00105-y

Jiang, G., Wei, Z., Xu, J., Chen, H., Zhang, Y., She, X., ... Liao, B. 2017. Bacterial wilt in China: history, current status, and future perspectives. *Front. Plant Sci*. **8:** 1549.doi.org/10.3389/fpls.2017.01549

Jiang, D., Zeng, Q., Banerjee, B., Lin, H., Srok, J., Yu, M.,Yang, C. H. 2022. The phytopathogen *Dickeyadadantii* 3937 cpxR locus gene participates in the regulation of virulence and the global c di GMP network. *Mol. Plant Pathol*. **23**: 1187-1199.doi.org/10.1111/mpp.13219

Islam, T., Haque, M. A., Barai, H. R., Istiaq, A.,Kim, J. J. 2024. Antibiotic resistance in plant pathogenic bacteria: recent data and environmental impact of unchecked use and the potential of biocontrol agents as an eco-friendly alternative. *Plants* 13: 1135.doi.org/10.3390/plants13081135

Kharadi, R. R., Schachterle, J. K., Yuan, X., Castiblanco, L. F., Peng, J., Slack, S. M., ... Sundin, G. W. 2021. Genetic dissection of the *Erwinia amylovora* disease cycle. *Annu.Rev.Phytopathol*. **59**: 191-212.doi.org/10.1146/annurev-phyto-020620-095540

Li, Y., Dong, J.,Qin, J. J. 2024. Small molecule inhibitors targeting heat shock protein 90: An updated review. *Eur. J.Medicin. Chem*. *275*: 116562.doi.org/10.1016/j.ejmech.2024.116562

Mahato, T., Mandal, J., Chatterjee, E., Bhattacharya, S.,Sinha, S. 2025. Subtractive genome mining in Xanthomonas citri pv. citri strain 306 for identifying novel drug target proteins coupled with in-depth protein-protein interaction and coevolution analysis-A leap towards prospective drug design. *Biochemic.Biophysic. Res.Commu*. **747**: 151289.doi.org/10.1016/j.bbrc.2025.151289

Maisuria, V. B.,Nerurkar, A. S. 2013. Characterization and differentiation of soft rot causing *Pectobacteriumcarotovorum* of Indian origin. *Eur. J.Plant Pathol*.**136**: 87-102.doi.org/10.1007/s10658-012-0140-0

Mitra, P., Singha, S., Roy, P., Saha, D.,Chatterjee, S. 2024. A molecular docking study between heavy metals and hydrophilic Hsp70 protein to explore binding pockets. *J. Proteins and Proteo*. **15**: 413-428.doi.org/10.1007/s42485-024-00150-y

Mulungu, E. 2024. Unmasking the hidden threat: a review of damage and losses due to phytopathogenic bacteria. *J. Curr.Opin. Crop Sci*. **5**: 250-263.doi.org/10.62773/jcocs.v5i4.277

Munyaneza, J. E.,Bizimungu, B. 2022. Management of potato pests and diseases in Africa. *Ins.Pests of Potato*, 407-426.https://doi.org/10.1016/B978-0-12-821237-0.00016-0

Sharma, D., Bisht, D. 2017. Role of bacterioferritin & ferritin in M. tuberculosis pathogenesis and drug resistance: a future perspective by interactomic approach. *Front.Cellu.Infect. Microbiol.* **7**: 240.doi.org/10.3389/fcimb.2017.00240

Shiau, A. K., Harris, S. F., Southworth, D. R., Agard, D. A. 2006. Structural analysis of E. coli hsp90 reveals dramatic nucleotide-dependent conformational rearrangements. *Cell* 127: 329-340.DOI 10.1016/j.cell.2006.09.027

Sicard, A., Zeilinger, A. R., Vanhove, M., Schartel, T. E., Beal, D. J., Daugherty, M. P., Almeida, R. P. 2018. Xylella fastidiosa: insights into an emerging plant pathogen. *Annu. Rev. Phytopathol*. **56**: 181-202.doi.org/10.1146/annurev-phyto-080417-045849

Sievers, F., Wilm, A., Dineen, D., Gibson, T. J., Karplus, K., Li, W., ... & Higgins, D. G. 2011. Fast, scalable generation of high quality protein multiple sequence alignments using Clustal Omega. *Mol.Systems Biol*.**539**.doi.org/10.1038/msb.2011.75

Tessema, G. L., & Seid, H. E. 2023. Potato bacterial wilt in Ethiopia: history, current status, and future perspectives. *PeerJ*.**11**: e14661.DOI:10.7717/peerj.14661

Verma, R. K., Biswas, A., Kakkar, A., Lomada, S. K., Pradhan, B. B., Chatterjee, S. 2020. A bacteriophytochrome mediates interplay between light sensing and the second messenger cyclic di-GMP to control social behavior and virulence. *Cell Reports*, **32**:doi.org/10.1016/j.celrep.2020.108202

Wang, Z., Luo, W., Cheng, S., Zhang, H., Zong, J., Zhang, Z. 2023. *Ralstonia solanacearum*–a soil borne hidden enemy of plants: research development in management strategies, their action mechanism and challenges. Front. Plant Sci. 14: 1141902.doi.org/10.3389/fpls.2023.1141902

Wang, Y., Ma, W., Zheng, W. 2013. Deguelin, a novel anti-tumorigenic agent targeting apoptosis, cell cycle arrest and anti-angiogenesis for cancer chemoprevention. *Mol.Clinic. Oncol*. **1:** 215-219.doi.org/10.3892/mco.2012.36

Wickner, S., Nguyen, T. L. L., Genest, O. 2021. The bacterial Hsp90 chaperone: cellular functions and mechanism of action. *Annu.Rev.Microbiol*. **75**: 719-739.doi.org/10.1146/annurev-micro-032421-035644

Wright, P. E.,Dyson, H. J. 1999. Intrinsically unstructured proteins: re-assessing the protein structure-function paradigm. *J.Mol.Biol.* **293**:321-331.doi.org/10.1006/jmbi.1999.3110

Yadav, P. K., Singh, G., Gautam, B., Singh, S., Yadav, M., Srivastav, U., Singh, B. 2013. Molecular modeling, dynamics studies and virtual screening of Fructose 1, 6 biphosphate aldolase-II in community acquired-methicillin resistant Staphylococcus aureus (CA-MRSA). *Bioinformation* **9**: 158.doi: 10.6026/97320630009158

Zhou-qi, C., Bo, Z. H. U., Guan-lin, X., Bin, L., Shi-wen, H. 2016. Research status and prospect of Burkholderia glumae, the pathogen causing bacterial panicle blight. *Rice Sci.* **23**: 111-118.doi.org/10.1016/j.rsci.2016.01.007